www.nature.com/mtm

ARTICLE

Quantitative, noninvasive, *in vivo* longitudinal monitoring of gene expression in the brain by co-AAV transduction with a PET reporter gene

Sea Young Yoon[1], Carlos Gay-Antaki[1], Datta E Ponde[2,5], Harish Poptani[2], Charles H Vite[3] and John H Wolfe[1,3,4]

In vivo imaging of vector transgene expression would be particularly valuable for repetitive monitoring of therapy in the brain, where invasive tissue sampling is contraindicated. We evaluated adeno-associated virus vector expression of a dopamine-2 receptor (D2R) mutant (D2R80A) by positron emission tomography in the brains of mice and cats. D2R80A is inactivated for intracellular signaling and binds subphysiologic amounts of the radioactive [18F]-fallypride analog of dopamine. The [18F]-fallypride signal bound to D2R80A in the injection site was normalized to the signal from endogenous D2R in the striatum and showed stable levels of expression within individual animals. A separate adeno-associated virus type 1 vector with identical gene expression control elements, expressing green fluorescent protein or a therapeutic gene, was coinjected with the D2R80A vector at equal doses into specific sites. Both transgenes had similar levels of gene expression by immunohistochemistry, *in situ* hybridization, and quantitative PCR assays, demonstrating that D2R80A is a faithful surrogate measure for expression of a gene of interest. This dual vector approach allows the D2R80A gene to be used with any therapeutic gene and to be injected into a single site for monitoring while the therapeutic gene can be distributed more widely as needed in each disease.

INTRODUCTION

A number of imaging technologies are available for studying gene expression in living subjects. Approaches using optical imaging of reporter genes such as green fluorescent protein (GFP)[1] and luciferase[2–5] are widely used in rodents but are limited to small animals due to attenuation of visible light photons especially in deep tissues. Magnetic resonance imaging and positron emission tomography (PET) imaging allow visualization of tissues at greater depths and are thus applicable to larger animals and humans. With repetitive imaging, both modalities can provide data on persistence of the vector. Some magnetic resonance imaging and PET imaging reporter genes may be extended directly into clinical human applications as many clinically approved reagents are in use.[6,7] Magnetic resonance imaging can provide high-resolution tomographic imaging of gene expression but has relatively low sensitivity, whereas PET has very high sensitivity, making it potentially useful for detecting the relatively low levels of gene expression after vector transfer.[8–11] PET imaging can also be quantitative, enabling measurement of intensity and regional distribution of the expressed gene.

Several PET reporter gene systems have been developed. They involve the binding of a reporter gene with a specific radiolabeled probe, thus the level of measured radioactivity reflects the expression level of the reporter gene. PET reporter genes used to image gene expression include herpes simplex virus type 1 thymidine kinase (HSV1-tk),[12–15] dopamine-2 receptor (D2R),[14,16] D2R mutant,[9] type 2 cannabinoid receptor mutant,[17] sodium iodide symporter,[18] and the somatostatin receptor 2.[19–24] The D2R80A reporter is a D2R mutant that has been used to image gene transfer after viral vector gene delivery in mouse liver[9] and rat heart using the PET ligand [18F]-spiperone[25] and in human glioma cells in mouse subcutaneous xenografts using [11C]-raclopride.[26] The D2R80A receptor has a number of desirable features for use as a reporter gene in the brain[11]: (i) it is a mammalian protein and thus nonimmunogenic in clinical application; (ii) it has been inactivated for downstream intracellular signaling, with the mutation in the cytoplasmic domain[9] and thus is biologically inert in cells that do not normally express the D2R gene; (iii) the radiolabeled ligands for this receptor cross the blood–brain barrier[16]; and (iv) radiolabeled ligand binding is detectable at subphysiological concentrations, which avoids triggering undesirable activity in cells that normally express the D2R gene.[27–30]

[1]Research Institute of Children's Hospital of Philadelphia, Philadelphia, Pennsylvania, USA; [2]Department of Radiology, Perelman School of Medicine, University of Pennsylvania, Philadelphia, Pennsylvania, USA; [3]W.F. Goodman Center for Comparative Medical Genetics, School of Veterinary Medicine, University of Pennsylvania, Philadelphia, Pennsylvania, USA; [4]Department of Pediatrics, Perelman School of Medicine, University of Pennsylvania, Philadelphia, Pennsylvania, USA; [5]Current address: Deccan Institute of Chemical Technology, Maharashtra, India. Correspondence: JH Wolfe (jhwolfe@vet.upenn.edu)

Despite its several desirable features, the potential of D2R80A as a PET reporter gene in the brain has not been investigated. In this study, the D2R80A PET-based receptor–ligand binding system was evaluated to monitor the distribution, magnitude, and duration of adeno-associated virus (AAV)-mediated expression. We used the [18F]-fallypride ligand, which has a higher binding affinity to D2R than [18F]-spiperone.[31] We assessed the potential of D2R80A as a surrogate for another gene by coinjection of a separate AAV vector expressing GFP in the mouse brain. To evaluate its potential in a preclinical setting, the D2R80A vector was tested in the cat brain, coinjected with an equal dose of AAV vector expressing a candidate therapeutic gene, feline α-mannosidase (fMANB), an enzyme deficient in the lysosomal storage disorder, α-mannosidosis.[32] Expression levels of both vectors were similar quantitatively, indicating that the PET reporter would be a faithful surrogate for a therapeutic vector. Furthermore, the level of D2R80A gene expression was evaluated relative to the internal standard of ligand binding in the striatum (caudate-putamen), which provided a control for variations of uptake and crossing the blood–brain barrier in individual animals and with different preparations of the radioligand. The level of gene expression within individual animals was sustained at similar levels for 3–6 months.

RESULTS

[18F]-Fallypride binding in the brain following intraventricular injection of AAV1.D2R80A in neonatal mice

Intraventricular injection of neonatal mice with AAV1 results in widespread transduction of cells in the neocortex, the entorhinal cortex, and the hippocampus.[33] Four weeks following neonatal injection with AAV1.D2R80A into the cerebral lateral ventricles, mice ($n = 5$) were imaged by PET with [18F]-fallypride to examine the binding pattern in the brain. PET imaging revealed [18F]-fallypride accumulation in the striatum where endogenous D2R is expressed, and throughout the cortical regions of the mouse brains (Figure 1a), indicating expression of D2R80A. In the transverse view, portions of the striatum and the cortex are superimposed, thus the [18F]-fallypride signal appear to overlap, but separation of the two regions is apparent in the coronal view.

No evidence of adverse reaction was observed following vector or probe injection in mice. Iba1 (microglia marker) and GFAP (astrocytic marker) immunostaining were done on the brain sections as described previously,[34] which showed that no inflammatory reaction or reactive gliosis were present at the time of euthanasia (Supplementary Figure S1b,d). Mean radioactivity was measured from an ellipsoid region of interest from the cortex of each hemisphere relative to [18F]-fallypride binding in the striatum. [18F]-fallypride accumulation in the striatum was used as a baseline to report relative activity in extrastriatal regions. In the cortex of vector-injected brains, 33.7–90.5% mean radioactivity relative to striatum was detected (Figure 1b).

Serial PET imaging following intraparenchymal injection of AAV1.D2R80A in adult mice

Adult mice ($n = 6$) were coinjected unilaterally with equivalent doses (1.5×10^{10} GC) of AAV1.D2R80A and AAV1.GFP into the cerebellum at a site distal to the striatum where there is no endogenous D2R expressed. A second group of mice ($n = 4$) was given multiple injections of AAV1.D2R80A and AAV1.GFP (2×10^{10} GC per site) into the hippocampus and thalamus in one hemisphere and the cerebellum in the opposite hemisphere. Serial PET studies were performed monthly for up to 3 months postinjection in
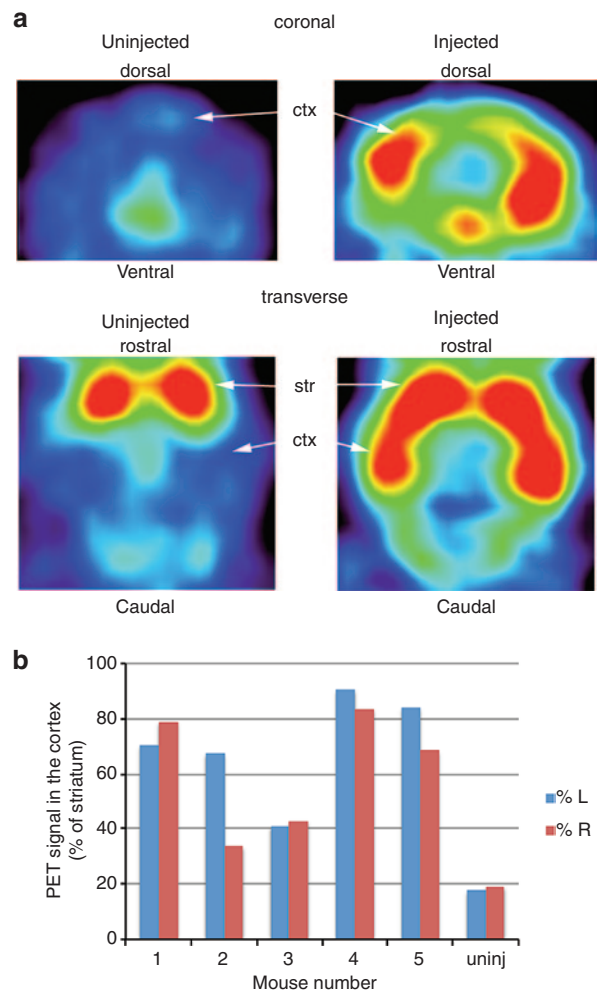

Figure 1 Positron emission tomography (PET) signal in the mouse cortex following bilateral intraventricular vector injection in neonatal mice. (**a**) Neonatal mice ($n = 5$) were injected bilaterally into the lateral ventricles with equivalent titers (9×10^9 GC) of AAV1.D2R80A and AAV.GFP and then imaged 4 weeks postinjection by PET with [18F]-fallypride. (**b**) Mean radioactivity in the cortex of each animal was measured by quantifying [18F]-fallypride binding in the cortex relative to binding in the striatum. AAV, adeno-associated virus; Ctx, cortex; GFP, green fluorescent protein; L, left hemisphere; R, right hemisphere; str, striatum; uninj, uninjected.

the same animals to assess persistence of gene expression and detection by [18F]-fallypride binding. In the first group of mice, imaging indicated [18F]-fallypride accumulation in the cerebellum in the injected hemisphere, whereas [18F]-fallypride binding was only detected in the striatum of the uninjected mouse brain (Figure 2a). The sagittal view of the image also shows radioactivity in the harderian glands (located in the orbital cavity), which accumulates tracers nonspecifically.[35–37] Radiotracer accumulates nonspecifically outside the brain in the harderian glands, salivary glands, nasal cavity, and orbital cavity as well as the spinal column.

PET imaging of the second group of mice showed [18F]-fallypride activity in the hippocampus and thalamus of the left hemisphere and the cerebellum of the right hemisphere (Figure 2b). D2R80A expression in the injected regions was measured by quantifying [18F]-fallypride binding monthly, for 3 months postinjection, in both groups (Figure 2c–e). Higher levels of radioactivity were detected in
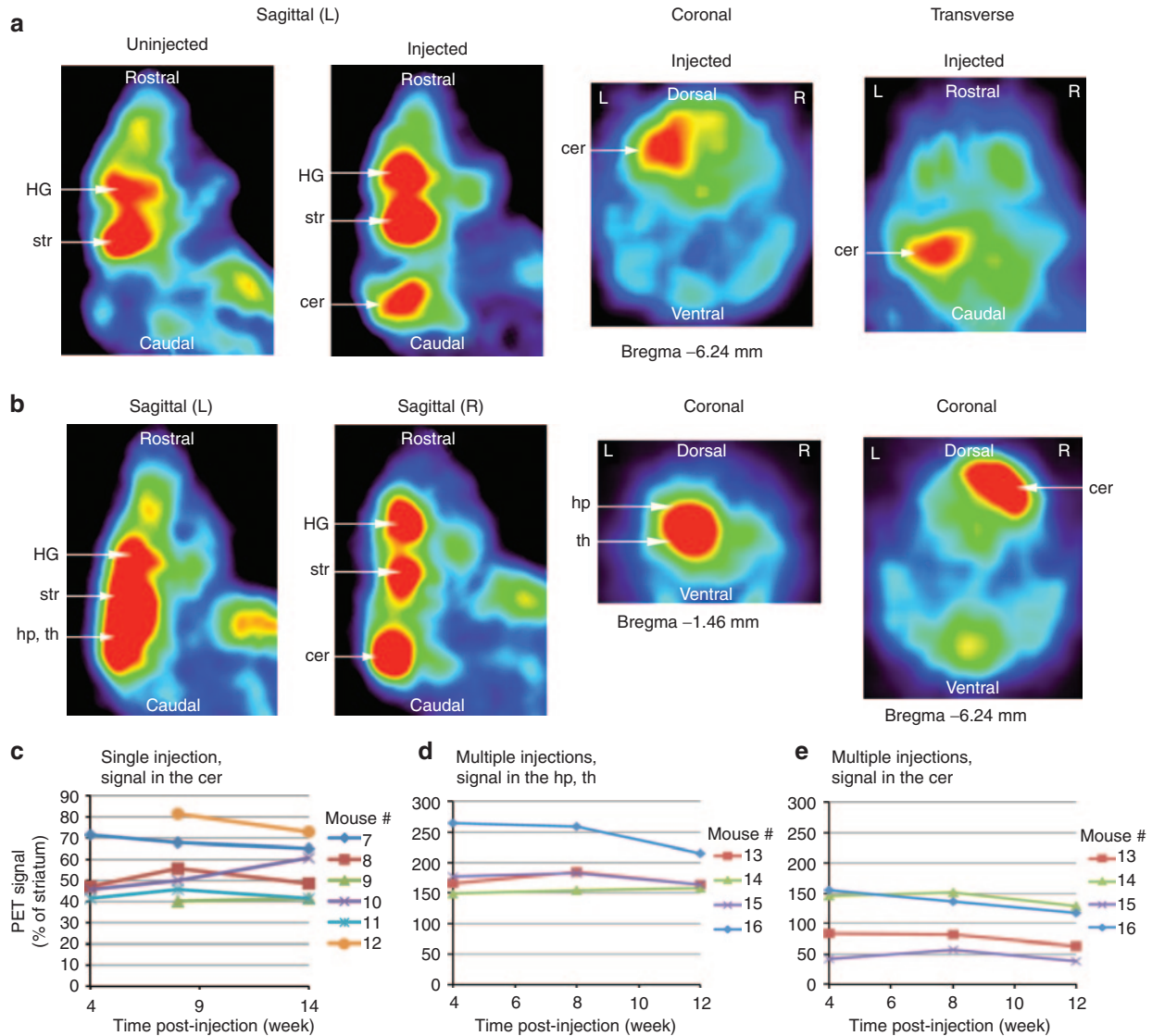
Figure 2 Serial positron emission tomography (PET) imaging following intraparenchymal injection of AAV1.D2R80A in adult mice. (**a**) Adult mice ($n = 6$) were coinjected unilaterally with equivalent titers (1.5×10^{10} GC) of AAV1.D2R80A and AAV1.GFP into the cerebellum of the left hemisphere. (**b**) A second group of mice ($n = 4$) was given multiple injections of AAV1.D2R80A and AAV1.GFP (2×10^{10} GC per site) into the hippocampus and thalamus in the left hemisphere and the cerebellum in the right hemisphere. Serial PET studies were performed in both groups monthly up for 3 months postinjection. PET signal was measured in each animal at each time point by quantifying [^{18}F]-fallypride binding relative to the striatum in: (**c**) the cerebellum following a single unilateral injection and (**d**) the hippocampus and thalamus and (**e**) the cerebellum following multiple injections in the second group of mice. AAV, adeno-associated virus; Cer, cerebellum; GFP, green fluorescent protein; HG, harderian gland; hp, hippocampus; L, left hemisphere; R, right hemisphere; str, striatum; th, thalamus.

the second group of animals (Figure 2d,e), which were injected with higher titer vectors. No significant decrease in signal was observed over the 3-month period indicating continued D2R80A expression and suggesting that no adverse immune response against the reporter gene had occurred. Iba1 (microglia marker) and GFAP (astrocytic marker) immunostaining were done on the brain sections, which showed that no inflammatory reaction or reactive gliosis had occurred (Supplementary Figure S1b,d).

Correlation of reporter PET signal with the reporter gene expression in mouse brains
Following PET imaging at the last time point, the mice were perfused and the brains were analyzed by *in situ* hybridization using D2R80A-specific probes and immunofluorescence using anti-D2R antibody. D2R80A expression seen by [^{18}F]-fallypride binding in PET

imaging correlated well with D2R80A mRNA and protein expression in all animals. Specific D2R80A expression was observed in the hippocampus and thalamus of the injected hemisphere, and the GFP-positive areas seen by *in situ* hybridization and fluorescence also correlated well with the PET imaging results (Figure 3a). Mice injected into the cerebellum showed exclusive D2R80A mRNA and protein expression in the injected hemisphere of the cerebellum, and this also correlated well with the GFP expression (Figure 3b).

The brains were analyzed by real-time quantitative PCR for quantification of viral vector genome copies. D2R80A vector genome copies were measured in triplicate gDNA samples, and the results were normalized to the levels of GAPDH in each sample in order to correct variations in nucleic acid quality and quantity. The PET signal correlated well with the vector genome copy numbers in the brain of animals that received a single unilateral cerebellar vector
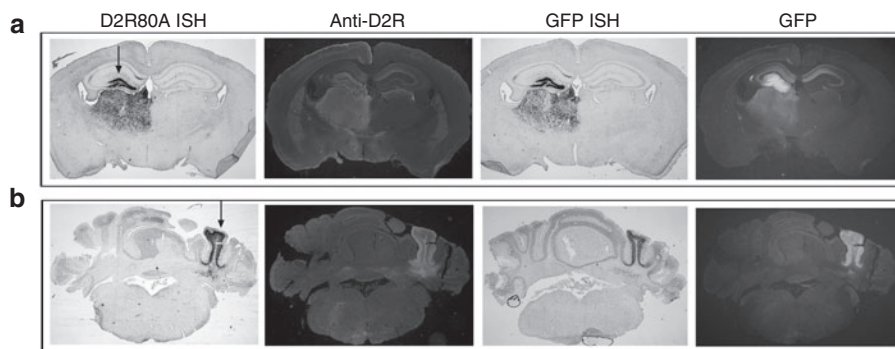
Figure 3 Coexpression of D2R80A and green fluorescent protein (GFP) vectors in the mouse brain. Following positron emission tomography imaging, mice were euthanized for *in situ* hybridization and immunofluorescence to detect D2R80A mRNA, dopamine-2 receptor, GFP mRNA, and GFP in the: (**a**) hippocampus and thalamus and (**b**) cerebellum. The injection sites are shown with arrows on the D2R80A *in situ* hybridization sections.

injection (Figure 4a, $R^2 = 0.80$, $P < 0.05$) as well as those injected into the thalamus, hippocampus, and cerebellum (Figure 4b, $R^2 = 0.92$, $P < 0.001$). Increasing PET signal was observed with increasing levels of viral vector genome copy number in the brains, suggesting [18F]-fallypride binding as a good indicator of the vector delivery and reporter gene expression.

In vivo PET imaging of vector-mediated D2R80A expression in the cat brain

To assess D2R80A as a surrogate marker for a therapeutic gene in the significantly larger cat brain, two separate AAV1 vectors, one to express D2R80A and the other to express feline MANB, were constructed under the control of the human GUSB gene promoter.[38] Both vectors were coinjected into cats ($n = 3$) along two injection tracks (at 1.9×10^{10} GC for each vector at each injection point in the column), unilaterally into the cortex, hippocampus, and thalamus. *In vivo* PET imaging was performed at 9, 16, and 24 weeks postinjection. [18F]-fallypride accumulation was observed in the two discrete injection tracts posterior to the striatum on the injected side of the brain (Figure 5a). The [18F]-fallypride signal from the vector-mediated D2R80A expression was clearly distinguishable, by location, from the endogenous D2R expression in the striatum. The [18F]-fallypride bound exclusively to the endogenous D2R in the striatum in the uninjected side of the brain (with nonspecific signal visible in the periorbital sinus near the eye).

Mean radioactivity in the injected brain regions was quantified at each time point. The data showed continuous expression and detection by [18F]-fallypride binding of the vector-mediated reporter gene for up to 6 months postinjection, when the cats were euthanized. Mean radioactivity in the brain varied from 27.5 to 45.3% relative to activity in the striatum (Figure 5b). Positive signals were seen at all time points and in all animals, indicating continued D2R80A expression. As in the mice, no evidence of adverse reaction was observed following vector or probe injection in cats. Iba1 (microglia marker) and GFAP (astrocytic marker) immunostaining were done on the cat brain sections, which showed that no inflammatory reaction or reactive gliosis had occurred (Supplementary Figure S1e,f).

Postmortem correlation of PET images and vector distribution in the cat brain

The vector genome copies present in the cat brain were determined by real-time quantitative PCR on the genomic DNA isolated from transverse sections of the cat brains and compared to the PET images at each corresponding level. To quantify the accumulation
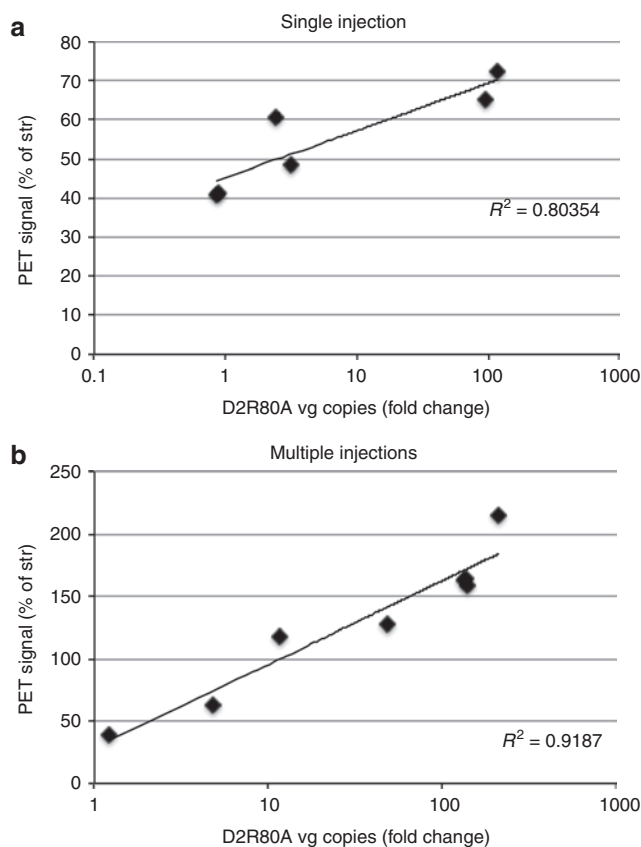

Figure 4 Correlation of reporter positron emission tomography (PET) signal with the vector genome copy numbers in the mouse brain. PET signal in the injected brain regions were correlated with the D2R80A vector genome copies in the brain, quantified by real-time quantitative PCR, and normalized to GAPDH expression following (**a**) a single unilateral cerebellar injection (at 14 weeks postinjection) and (**b**) multiple injections into the thalamus, hippocampus, and cerebellum (at 12 weeks postinjection). Str, striatum; vg, vector genome.

of [18F]-fallypride at each level, the mean radioactivity in the injected brain regions were calculated from a series of 5-mm-thick reconstructed transverse images (Figure 6a,b) for each cat. The calculations were based on the actual mean counts of radioactivity per voxel recorded in the regions of interest, whereas the intensity of the signal in the PET images (Figure 6a) was thresholded for each image to highlight where the signal was present. The mean radioactivity in the injected region for each transverse brain block was
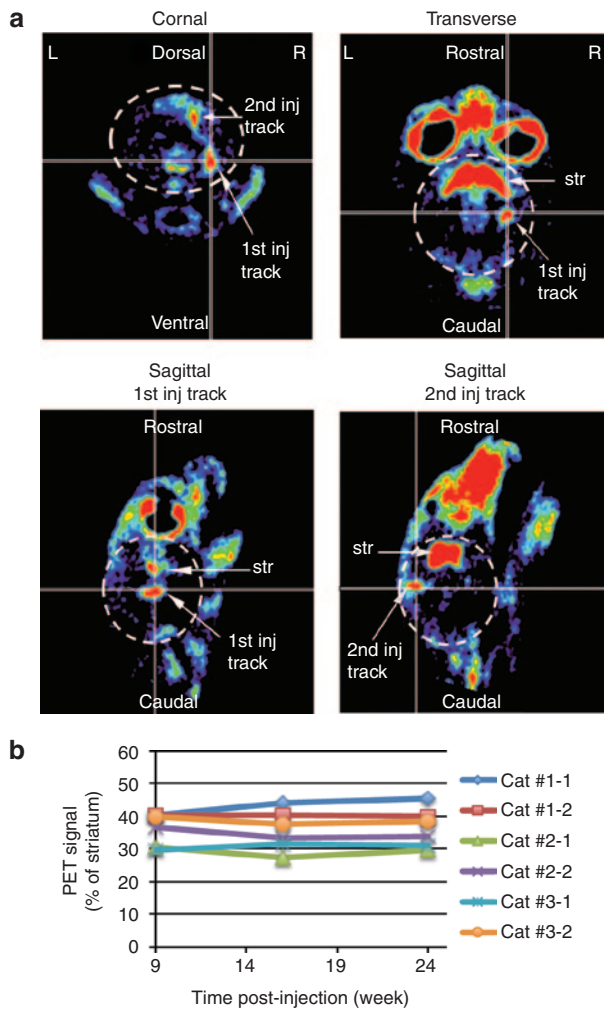
Figure 5 [18F]-fallypride accumulation in the cat brain following vector injection. Cats (*n* = 3) were stereotactically injected into the brain in two tracks of the right hemisphere with equivalent titers of AAV1.D2R80A and AAV1.fMANB (1.9×10^{10} GC per site along the track). Positron emission tomography imaging was performed at 9, 16, and 24 weeks postinjection. (**a**) [18F]-fallypride binding in the brain is shown in coronal, transverse, and sagittal views at 9 weeks. (**b**) Mean radioactivity in each injection track of cats was measured by quantifying [18F]-fallypride accumulation in the injected regions relative to the striatum. AAV, adeno-associated virus; fMANB, feline α-mannosidase; Str, striatum; L, left hemisphere; R, right hemisphere.

calculated relative to the activity in the whole striatum to provide a common denominator (Figure 6c). The change in D2R80A vector genome copies in each section correlated well with the PET signal in each transverse slice (Figure 6d, $R^2 = 0.78$, $P < 0.001$).

Correlation between reporter and therapeutic gene expression in the cat brain

The *in situ* hybridization-positive regions for D2R80A mRNA were present in the vector-injected regions and were located where [18F]-fallypride binding was detected by PET imaging (Figure 7a). *In situ* hybridization for expression of the coinjected vector expressing fMANB[32] were also positive in the same areas as the PET vector around the injection tracks of the cat brain (Figure 7a). Quantitative analysis of *in situ* hybridization results showed a good correlation between D2R80A and the fMANB therapeutic gene expression levels in the cat brain (Figure 7b, $R^2 = 0.93$, $P < 0.001$). The number of

vector genome copies of the fMANB vector also correlated well with the fold change in D2R80A vector genome copies (Figure 7c, $R^2 = 0.80$, $P < 0.001$), indicating that D2R80A was a faithful surrogate for measuring therapeutic gene delivery.

DISCUSSION

This study evaluated the ability of D2R80A to measure gene expression in the living brain, in the presence of endogenous D2 receptors, using the D2R-specific PET ligand [18F]-fallypride. The experiments show that the system allows noninvasive, repetitive monitoring of vector transferred gene expression in the brain *in vivo*. Furthermore, the data show that when injected into the same structure, the PET reporter is a faithful surrogate for the relative level of expression of another gene.

The advantage of using separate vectors, one to express the reporter gene and the other to express a therapeutic gene, is that the reporter gene activity is independent of the therapeutic gene and thus allows the D2R80A gene to be used with any therapeutic gene in other genetic diseases. The same promoter and vector elements used for both the reporter and therapeutic vector constructs provide the greatest likelihood that they will be coexpressed in specific cells and brain regions. The current study proves the feasibility of using two separate vectors by confirming correlation of the PET reporter gene with two different vectors, a reporter gene expressing GFP as well as a candidate therapeutic gene, feline MANB. IRES-based bicistronic vector can be used for expression of both the reporter and therapeutic gene in the same construct, but expression of the downstream gene is often reduced.[39] The dual vector approach also allows the D2R80A gene to be injected into a single site for monitoring while the therapeutic gene can be distributed more widely as needed in each disease.

The PET ligand [18F]-fallypride is widely used in animals and humans[27–30,40] due to its high affinity for dopamine D_2/D_3 receptors. Most importantly, it crosses the blood–brain barrier after intravenous injection, making it suitable for imaging the brain of patients. It is more sensitive than [11C]-raclopride,[41] with a detection threshold in the pM range compared with the nM range for the latter. Fallypride is also specific for dopamine receptors, whereas spiperone ([18F]-FESP), another D2R ligand used for imaging D2R80A in noncentral nervous system organs,[9,25] binds to serotonin as well as to dopamine receptors in the brain.[42] Fallypride has the desirable characteristics of short half-life and rapid clearance from nontarget tissues. It also is injected at subphysiological concentrations to avoid undesirable activation of D2 pathway in cells expressing the native receptor. It is approved for human use, which would facilitate future clinical usage of D2R80A as a reporter gene.

A consideration for using the D2R80A reporter system in the brain is the background expression level of the endogenously expressed D2R in the striatum (caudate-putamen). There is very little D3R present in the striatum and D2R/D3R expression in the extrastriatal brain regions is minimal.[31,41,43–45] As shown in our study, vector expression of D2R80A can be clearly distinguished from the endogenous D2R expression in the brain when injected at a site outside the striatum. This of course means we cannot monitor D2R80A expression in the striatum. However, a valuable advantage of having endogenous D2R expression in a discrete region is that it can be used as an internal binding control. In our study, using the endogenous D2R expression in the striatum of each animal as the baseline for comparison thus allowed the relative amount of reporter gene expression to be quantified in the injected brain regions. In addition, this corrected for animal-to-animal variation in probe delivery which can be
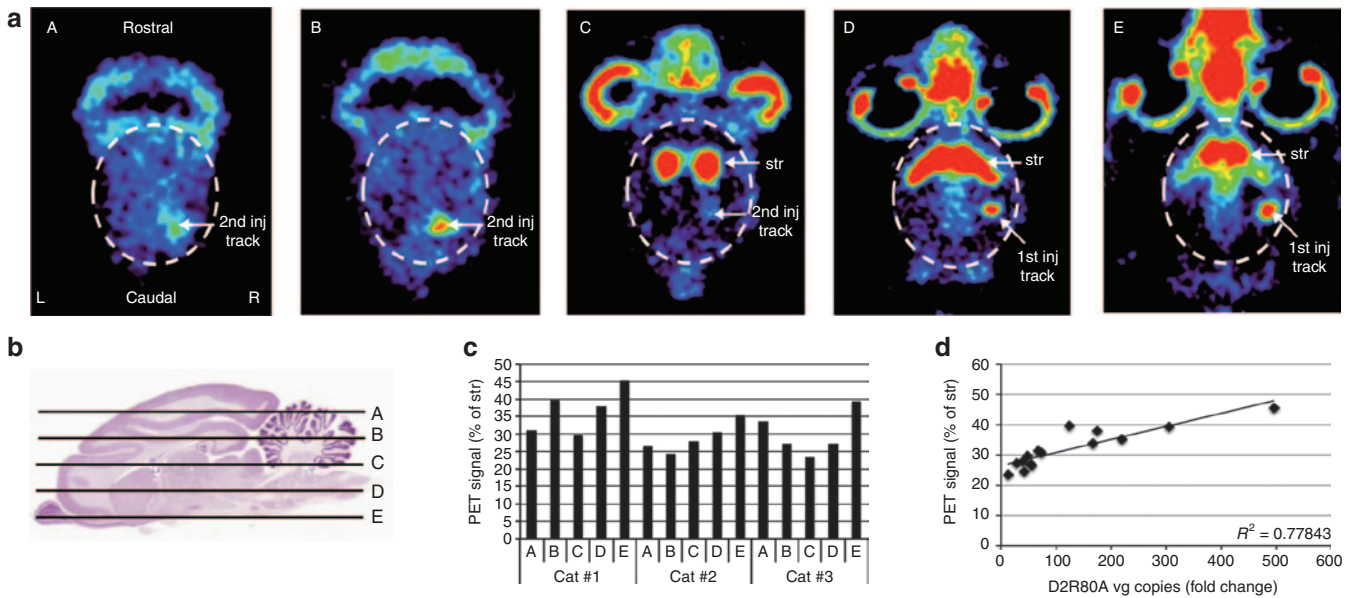
Figure 6 Correlation between [18F]-fallypride accumulation in the cat brain with the vector genome copy numbers. (**a**) Transverse positron emission tomography (PET) images with a thickness of 0.5 mm were reconstructed at 5-mm intervals from [18F]-fallypride imaging of cats at 24 weeks postinjection. Example images from cat #1 are shown. (**b**) Images shown in **a** correspond to the transverse brain blocks (A–E) shown. (**c**) The mean radioactivity (as % of striatum) was measured in each cat by quantifying the accumulation of [18F]-fallypride in the injected regions in each transverse brain block. PET signal in each brain block was calculated as a percentage of the activity in the whole striatum. Calculations are based on the actual mean counts of radioactivity per voxel recorded in the regions of interest and not based on the intensity of the signal in thresholded images shown in **a**. (**d**) PET signal in the injected brain regions were correlated with the D2R80A vector genome copies in the brain, quantified by real-time quantitative PCR, and normalized to GAPDH expression. Each data point represents each transverse block of the cat brain.
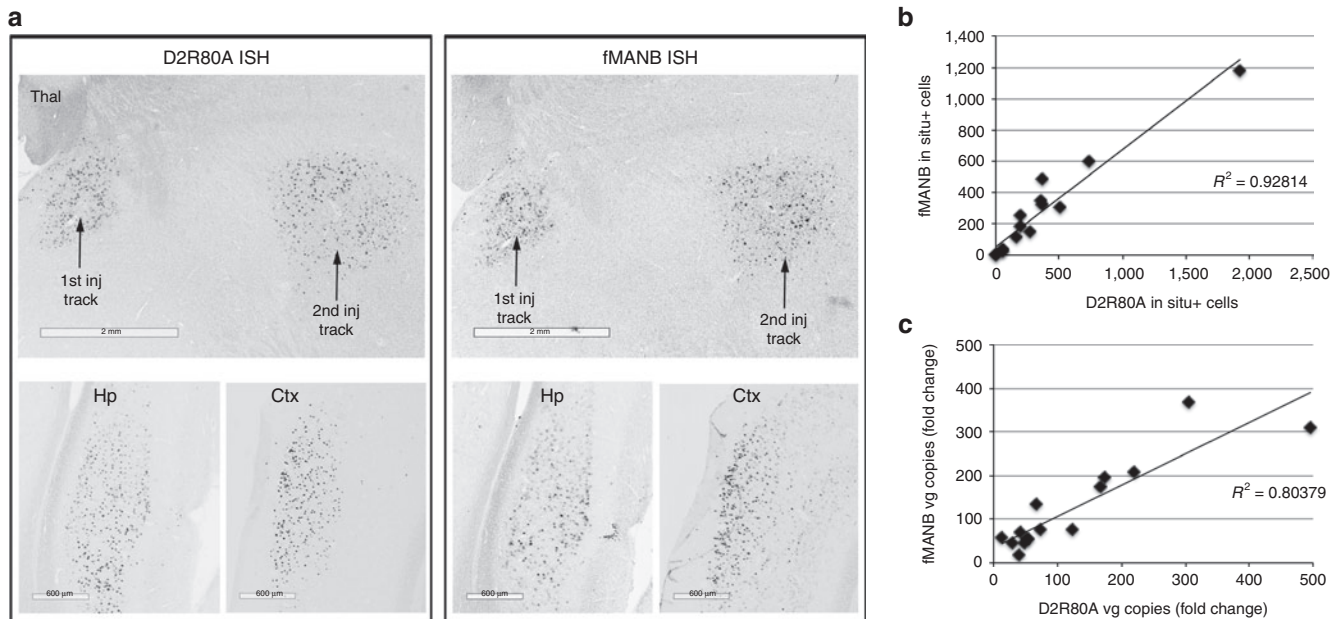

Figure 7 Coexpression of D2R80A and feline α-mannosidase (fMANB) vectors in the cat brain. Following positron emission tomography imaging, cats were euthanized and *in situ* hybridization was performed to detect D2R80A mRNA and fMANB mRNA on adjacent 20-μm cryosections from the transverse brain slices. (**a**) Examples of D2R80A mRNA- and fMANB mRNA-positive areas in the cat brain are shown. Bar (top) = 2 mm, (bottom) = 600 μm. (**b**) fMANB and D2R80A *in situ*-positive cells were quantified and correlated in each transverse brain section. (**c**) fMANB and D2R80A vector genome copy numbers were quantified by real-time quantitative PCR in each transverse brain section.

affected by the amount of the [18F]-fallypride actually being injected and getting into the brain due to variations with tail vein injection, which may result from either extravasation or adherence of tracer to the syringe. In future studies, [18F]-fallypride imaging will be performed in each subject prior to vector injection to measure baseline levels of endogenous D2R/D3R in the brain. The endogenous level

of D2R/D3R will then be used as a baseline to quantify relative levels of D2R80A expression in the injected brain region.

Other PET reporter genes have been developed for imaging gene expression in the brain, but each has disadvantages compared with D2R80A. A type 2 cannabinoid receptor (CB2) mutant was tested in rat striatum following transduction with bicistronic AAV vectors.[17]

CB_2 has low basal expression in the brain and it is normally expressed in the cerebellum and pons. However, its expression can be upregulated in inflammatory conditions by activated microglia,[46,47] which is a common feature in many neurodegenerative diseases and would interfere with the CB_2 reporter system. The HSV1-tk reporter gene system has been used to image gene expression in mouse models of human glioma in brain.[15] However, this system is limited to imaging the reporter gene in tumors as, currently, there are no probes available for the reporter protein that can cross the blood–brain barrier,[48] and incorporation of ganciclovir depends on cell division and thus is not applicable to most neurogenetic disease analyses. In addition, HSV1-tk is a foreign gene and may be immunogenic. Tk is also an intracellular reporter gene as opposed to membrane-bound reporter genes, which requires probes that can cross the cell membrane. Prior to the development of D2R80A mutant, adenoviral-mediated D2R overexpression in rat striatum was imaged using ^{11}C-labeled ligands.[49] This system could potentially be used for monitoring D2R expression in neurodegenerative diseases involving D2R replacement therapy in the striatum. However, ectopically expressed D2R could provoke adverse biological effects on transduced cells especially when long-term expression of the target gene is desired.

The D2R80A vectors can also be used to evaluate alternative routes of vector administration or different serotypes of AAV to improve biodistribution within the brain and used in combination with therapeutic vectors. Specific anatomical regions of ^{18}F-fallypride accumulation could be determined by combining PET imaging with magnetic resonance imaging. The dopamine receptor is relatively conserved in mammals and we did not find any evidence of an immune response to the rat D2R80A protein in mice or cats. Although a human D2R80A sequence would be used in human clinical trials, PET imaging is highly sensitive and the ligands are already approved for clinical use. This study shows that D2R80A imaging of vector gene expression is a faithful reporter for the expression of a therapeutic gene and thus should be a valuable surrogate for monitoring gene therapy of neurogenetic and other brain diseases.

MATERIALS AND METHODS

Experimental animals
Normal C3H mice (postnatal day 1 and 6–8 weeks old) produced in our breeding colony were used for experiments. All care and procedures were in accordance with the Institutional Animal Care and Use Committee at the Children's Hospital of Philadelphia.

Normal cats (7–8 weeks old) produced in the breeding colony of the veterinary school of the University of Pennsylvania were used for cat experiments. All care and procedures were in accordance with the Institutional Animal Care and Use Committee at the University of Pennsylvania.

Plasmids and AAV production
Rat D2R80A gene was obtained in Eco RI and Hind III restriction sites of pcDNA 3.1(+) backbone (Invitrogen) as a gift from S. Gambhir, Stanford University. The D2R80A gene was then cutout with Spe I and Apa I enzymes and recloned into the AAV packaging plasmid pZac2.1, provided by the Vector Core of the University of Pennsylvania. The vector genome contained AAV2 terminal repeats, a human GUSB promoter, simian virus 40 splice donor/acceptor signal, and bovine growth hormone polyadenylation signal. GFP and fMANB were also subcloned individually into pZac2.1 under the control of the human GUSB promoter. Recombinant AAV1 vectors were packaged by the University of Pennsylvania Vector Core following triple transfection of HEK293 cells by AAV cis-plasmid encoding the gene of interest, AAV trans-plasmid containing AAV rep and cap genes and adenovirus helper plasmid. Vectors were purified using iodixanol gradient ultracentrifugation, and the titers were determined by real-time PCR.[50] The infectivity of the packaged AAV vectors was verified by transduction of HEK293 cells and the specific protein expression was confirmed using immunocytochemistry *in vitro* (data not shown).

Vector injections
Intraventricular injection of neonatal mice. Neonatal C3H mice were cryoanesthetized and injected bilaterally into the lateral ventricles with equivalent titers (9×10^9 GC in 2 µl total injection volume) of AAV1 vectors expressing rat D2R80A and GFP with finely drawn glass micropipettes as described previously.[51]

Stereotaxic injections into adult mice. Adult C3H mice (6–8 weeks) were anesthetized, placed in a stereotaxic frame (David Kopf Instruments, Tujunga, CA) and injected unilaterally with 2–3 µl, equivalent titers of AAV1.D2R80A and GFP vectors ($1.5–2 \times 10^{10}$ GC) per site through burr holes made in the skull into the cerebellum alone or the cerebellum, thalamus, and hippocampus. The following injection coordinates were used: cerebellum (rostral-caudal: −6.64 mm, mediolateral: ±2 mm, dorsoventral: −0.8 mm); thalamus (rostral-caudal: −2 mm, mediolateral: ±1.5 mm, dorsoventral: −3.25 mm); and hippocampus (rostral-caudal: −2 mm, mediolateral: ±1.5 mm, dorsoventral: −1.62 mm) from Bregma.[52,53]

Stereotaxic injections into cats. Normal cats at 7–8 weeks of age were anesthetized, intubated, and placed in a stereotaxic head holder (David Kopf Instruments) for vector injection as described previously.[32] A 3-cm-long skin incision was made in the dorsal midline of the skin over the skull. Subcutaneous tissue was moved aside. A 25-gauge drill bit was used to drill a hole in the right side of the skull at the following positions: 0.5 cm lateral and 1.5 cm caudal to the bregma; and 1 cm lateral and 1.5 cm caudal to the bregma. A 25 µl, 29-gauge Hamilton syringe was filled with equivalent titers of AAV1.D2R80A and AAV1.fMANB. The needle was placed into the brain to the ventral-most limit and 3 µl of vectors, made up of 1.56 µl (1.9×10^{10} GC) of AAV1.D2R80A and 1.44 µl (1.9×10^{10} GC) of AAV1.fMANB, were injected at this site. Two minutes were allotted for brain diffusion. The needle was withdrawn 0.25 cm and the injection was repeated until out of the brain. The same procedure was completed for the second column. Approximately 30 µl of vectors were injected in total in each brain.

PET imaging
Imaging was performed using the Philips Mosaic HP Animal PET imaging system in the small animal imaging facility at the University of Pennsylvania. Mice were injected with 100–200 µCi of ^{18}F-fallypride, produced by the University of Pennsylvania's cyclotron facility, via the tail vein and anesthetized with 2–3% isoflurane in 1 l/minute of oxygen. After tracer uptake for 45 minutes, the mice were transferred to and scanned for 15 minutes on the animal bed of the small animal PET scanner (A-PET). Dynamics for ^{18}F-fallypride uptake in mice had previously been established by the A-PET facility. After the scan had finished, the mice were removed from the anesthesia and allowed to recover.

For the cats, a dynamic imaging protocol was used. The cats were anesthetized and placed onto a warming blanket on the PET scanner bed. The bed was moved into place with the head of the cat being centered in the field of view. The cats were injected with up to 3.5 mCi of ^{18}F-fallypride and imaged dynamically for 60 minutes (12 frames for 5 minutes per frame) starting at the time of injection, and the summed image from the 60-minute scan was used for data analysis. After the scans were completed, the animals were removed from the scanner and allowed to recover.

Data reconstruction was performed using a 3D-RAMLA protocol with decay correction turned on and normalization set for efficiency. The A-PET scanner produced images with a slice thickness of 0.5 mm, transverse imaging field of view at 12.8 cm and the approximate in-plane resolution of 2 mm. The imaging aperture of the A-PET scanner system is 20 cm and the axial length is 12 cm. Images were analyzed using AMIDE (http://amide.source-forge.net) on reconstructed images. 3D regions of interest were manually drawn over the injected brain regions to calculate the mean radioactivity using a calibration constant obtained from scanning a cylinder phantom in the scanner. These values were then converted to percentage of the radioactivity in the striatum, which serves as an internal positive binding control in the brain.

Tissue collection
Following PET imaging at the last time point, mice were euthanized and transcardially perfused with 4% paraformaldehyde. Cats were euthanized,

transcardially perfused with phosphate-buffered saline, and the brains were drop-fixed in 4% paraformaldehyde. Brains were then cryoprotected in 30% sucrose, embedded in optimum cutting temperature solution (Sakura, Torrance, CA), and then cryosectioned at 20 µm thickness using a cryostat (Leica Microsystems, Wetzlar, Germany). Mouse brains were cut coronally. Cat brains were sectioned (4–5 mm in thickness) in a dorsal plane as shown in Figure 6b and then further cryosectioned at 100 µm thickness for isolation of genomic DNA and 20 µm for *in situ* hybridization and immunofluorescent analysis. The sections were mounted on slides that were kept at −20 °C until processing.

Immunofluorescence

Sections were rinsed three times with phosphate buffer (0.1 mol/l, pH 7.4), incubated for 30 minutes at 80°C in sodium citrate buffer (10 mmol/l, pH 8.8), and retained in the solution to cool to room temperature. The slides were rinsed four times in Tris-buffered saline (0.1 mol/l Tris, pH 7.4, and 0.9% w/v NaCl) and incubated in blocking solution (10% fetal bovine serum, 4% goat serum, 0.5% Triton X-100 in Tris-buffered saline) for 1 hour at room temperature. The slides were then incubated overnight at 4 °C with the antidopamine D2 rabbit polyclonal antibody (AB5084P; Millipore, Temecula, CA) diluted at 1:100 in blocking solution. After four washes in Tris-buffered saline with 0.2% Triton X-100, the secondary antibody in blocking solution (1:250 dilution) was added for 1 hour before being washed four times in Tris-buffered saline. Slides were dried and coverslipped with VECTASHIELD Mounting Medium (Vector Laboratories, Burlingame, CA).

In situ hybridization

Sense and antisense DNA templates for RNA transcription were synthesized by PCR using D2R80A and fMANB sequence in the pZac2.1 plasmid, respectively, as the template with primers containing T7 or T3 RNA polymerase promoters upstream. Digoxigenin (DIG)-labeled RNA probes were produced using the DNA templates with the DIG RNA labeling kit (Roche Applied Science, Indianapolis, IN). The integrity and size of the labeled RNA probes were verified on a nondenaturing agarose gel and compared with the control RNA of the same length. Frozen sections were hybridized with DIG-labeled riboprobes specific for vector D2R80A or fMANB sequence, and DIG-positive cells were visualized by anti-DIG-alkaline phosphatase antibody (Roche) followed by NBT-BCIP substrate (Roche) for colorimetric detection of alkaline phosphatase. Whole slides were scanned using the Aperio scanscope (Aperio, Vista, CA). Images were converted to grayscale and the identical threshold was applied. The number of cells in the sections over the set threshold was counted by particle analysis using ImageJ software (NIH, Bethesda, MD).

Real-time PCR

Quantitative real-time PCR was used to determine the viral genome copies present in the brains. Every sixth coronal section was pooled from each mouse brain and the genomic DNA was extracted. For cat brains, genomic DNA was extracted from the 100-µm section of each transverse block and the vector genome copies quantified separately at each transverse level. Copies of D2R80A and fMANB vector genome were quantified using LightCycler FastStart DNA Master SYBR Green I mix (Roche) on a StepOne Real-Time PCR System (Applied Biosystems, Carlsbad, CA) and normalized to the GAPDH gene. For each gene assayed, triplicate samples derived from each DNA pool were used for quantification in mouse brains. Duplicate samples at each transverse level of the cat brains were used for quantification. For D2R80A vector genome quantification, the forward primer was designed to bind the GUSB promoter and the reverse primer bound to the D2R80A gene sequence. The primer sequences were as follows: forward: 5′-ACC TCC CGC GCT TTT CTT AG-3′, reverse: 5′-GCT CCA GTT CTG CCT CTC CA-3′. For fMANB vector genome quantification, the primer sequences were as follows: forward: 5′-GCC CAT GGA AAT CCG TAC CT-3′, reverse: 5′-TGC GAT GCA ATT TCC TCA TTT-3′.

Statistical analysis

Linear regression analysis was performed to assess the linear relationship between two variables. Pearson correlation coefficient (R^2) and P values were calculated to measure confidence and statistical significance of positive linear correlations shown, respectively. A P value of <0.05 was considered as statistically significant.

REFERENCES

1 Hoffman, RM and Yang, M (2006). Whole-body imaging with fluorescent proteins. *Nat Protoc* **1**: 1429–1438.

2 Gross, S and Piwnica-Worms, D (2005). Spying on cancer: molecular imaging *in vivo* with genetically encoded reporters. *Cancer Cell* **7**: 5–15.

3 Ilagan, MX, Lim, S, Fulbright, M, Piwnica-Worms, D and Kopan, R (2011). Real-time imaging of notch activation with a luciferase complementation-based reporter. *Sci Signal* **4**: rs7.

4 Rehemtulla, A, Stegman, LD, Cardozo, SJ, Gupta, S, Hall, DE, Contag, CH et al. (2000). Rapid and quantitative assessment of cancer treatment response using *in vivo* bioluminescence imaging. *Neoplasia* **2**: 491–495.

5 Contag, PR, Olomu, IN, Stevenson, DK and Contag, CH (1998). Bioluminescent indicators in living mammals. *Nat Med* **4**: 245–247.

6 Gilad, AA, Winnard, PT Jr, van Zijl, PC and Bulte, JW (2007). Developing MR reporter genes: promises and pitfalls. *NMR Biomed* **20**: 275–290.

7 Peñuelas, I, Mazzolini, G, Boán, JF, Sangro, B, Martí-Climent, J, Ruiz, M et al. (2005). Positron emission tomography imaging of adenoviral-mediated transgene expression in liver cancer patients. *Gastroenterology* **128**: 1787–1795.

8 Jacobs, AH, Winkler, A, Castro, MG and Lowenstein, P (2005). Human gene therapy and imaging in neurological diseases. *Eur J Nucl Med Mol Imaging* **32** (suppl. 2): S358–S383.

9 Liang, Q, Satyamurthy, N, Barrio, JR, Toyokuni, T, Phelps, MP, Gambhir, SS et al. (2001). Noninvasive, quantitative imaging in living animals of a mutant dopamine D2 receptor reporter gene in which ligand binding is uncoupled from signal transduction. *Gene Ther* **8**: 1490–1498.

10 Waerzeggers, Y, Monfared, P, Viel, T, Winkeler, A, Voges, J and Jacobs, AH (2009). Methods to monitor gene therapy with molecular imaging. *Methods* **48**: 146–160.

11 Wolfe, JH, Acton, PD, Poptani, H and Vite, CH (2006). Molecular imaging of gene therapy for neurogenetic diseases. In: Kaplitt, M and During, M (eds). *Gene Therapy in the Central Nervous System: From Bench to Bedside*. Academic Press: San Diego, CA. pp. 335–350.

12 Gambhir, SS, Bauer, E, Black, ME, Liang, Q, Kokoris, MS, Barrio, JR et al. (2000). A mutant herpes simplex virus type 1 thymidine kinase reporter gene shows improved sensitivity for imaging reporter gene expression with positron emission tomography. *Proc Natl Acad Sci U S A* **97**: 2785–2790.

13 Tjuvajev, JG, Avril, N, Oku, T, Sasajima, T, Miyagawa, T, Joshi, R et al. (1998). Imaging herpes virus thymidine kinase gene transfer and expression by positron emission tomography. *Cancer Res* **58**: 4333–4341.

14 Ray, P, Bauer, E, Iyer, M, Barrio, JR, Satyamurthy, N, Phelps, ME et al. (2001). Monitoring gene therapy with reporter gene imaging. *Semin Nucl Med* **31**: 312–320.

15 Hospers, GA, Calogero, A, van Waarde, A, Doze, P, Vaalburg, W, Mulder, NH et al. (2000). Monitoring of herpes simplex virus thymidine kinase enzyme activity using positron emission tomography. *Cancer Res* **60**: 1488–1491.

16 MacLaren, DC, Gambhir, SS, Satyamurthy, N, Barrio, JR, Sharfstein, S, Toyokuni, T et al. (1999). Repetitive, non-invasive imaging of the dopamine D2 receptor as a reporter gene in living animals. *Gene Ther* **6**: 785–791.

17 Vandeputte, C, Evens, N, Toelen, J, Deroose, CM, Bosier, B, Ibrahimi, A et al. (2011). A PET brain reporter gene system based on type 2 cannabinoid receptors. *J Nucl Med* **52**: 1102–1109.

18 Groot-Wassink, T, Aboagye, EO, Wang, Y, Lemoine, NR, Reader, AJ and Vassaux, G (2004). Quantitative imaging of Na/I symporter transgene expression using positron emission tomography in the living animal. *Mol Ther* **9**: 436–442.

19 Kundra, V, Mannting, F, Jones, AG and Kassis, AI (2002). Noninvasive monitoring of somatostatin receptor type 2 chimeric gene transfer. *J Nucl Med* **43**: 406–412.

20 Rogers, BE, Parry, JJ, Andrews, R, Cordopatis, P, Nock, BA and Maina, T (2005). MicroPET imaging of gene transfer with a somatostatin receptor-based reporter gene and (94m) Tc-Demotate 1. *J Nucl Med* **46**: 1889–1897.

21 Singh, SP, Yang, D, Ravoori, M, Han, L and Kundra, V (2009). *In vivo* functional and anatomic imaging for assessment of *in vivo* gene transfer. *Radiology* **252**: 763–771.

22 Zinn, KR, Buchsbaum, DJ, Chaudhuri, TR, Mountz, JM, Grizzle, WE and Rogers, BE (2000). Noninvasive monitoring of gene transfer using a reporter receptor imaged with a high-affinity peptide radiolabeled with 99mTc or 188Re. *J Nucl Med* **41**: 887–895.

23 Zinn, KR and Chaudhuri, TR (2002). The type 2 human somatostatin receptor as a platform for reporter gene imaging. *Eur J Nucl Med Mol Imaging* **29**: 388–399.

24 Cotugno, G, Aurilio, M, Annunziata, P, Capalbo, A, Faella, A, Rinaldi, V *et al.* (2011). Noninvasive repetitive imaging of somatostatin receptor 2 gene transfer with positron emission tomography. *Hum Gene Ther* **22**: 189–196.

25 Chen, IY, Wu, JC, Min, JJ, Sundaresan, G, Lewis, X, Liang, Q *et al.* (2004). Micro-positron emission tomography imaging of cardiac gene expression in rats using bicistronic adenoviral vector-mediated gene delivery. *Circulation* **109**: 1415–1420.

26 Kummer, C, Winkeler, A, Dittmar, C, Bauer, B, Rueger, MA, Rueckriem, B *et al.* (2007). Multitracer positron emission tomographic imaging of exogenous gene expression mediated by a universal herpes simplex virus 1 amplicon vector. *Mol Imaging* **6**: 181–192.

27 Vandehey, NT, Moirano, JM, Converse, AK, Holden, JE, Mukherjee, J, Murali, D *et al.* (2010). High-affinity dopamine D2/D3 PET radioligands ^{18}F-fallypride and ^{11}C-FLB457: a comparison of kinetics in extrastriatal regions using a multiple-injection protocol. *J Cereb Blood Flow Metab* **30**: 994–1007.

28 Mukherjee, J, Christian, BT, Narayanan, TK, Shi, B and Collins, D (2005). Measurement of d-amphetamine-induced effects on the binding of dopamine D-2/D-3 receptor radioligand, ^{18}F-fallypride in extrastriatal brain regions in non-human primates using PET. *Brain Res* **1032**: 77–84.

29 Mukherjee, J, Yang, ZY, Das, MK and Brown, T (1995). Fluorinated benzamide neuroleptics–III. Development of (S)-N-[(1-allyl-2-pyrrolidinyl)methyl]-5-(3-[^{18}F]fluoropropyl)-2, 3-dimethoxybenzamide as an improved dopamine D-2 receptor tracer. *Nucl Med Biol* **22**: 283–296.

30 Narendran, R, Frankle, WG, Mason, NS, Rabiner, EA, Gunn, RN, Searle, GE *et al.* (2009). Positron emission tomography imaging of amphetamine-induced dopamine release in the human cortex: a comparative evaluation of the high affinity dopamine D2/3 radiotracers [^{11}C]FLB 457 and [^{11}C]fallypride. *Synapse* **63**: 447–461.

31 Vučković, MG, Li, Q, Fisher, B, Nacca, A, Leahy, RM, Walsh, JP *et al.* (2010). Exercise elevates dopamine D2 receptor in a mouse model of Parkinson's disease: *in vivo* imaging with [^{18}F]fallypride. *Mov Disord* **25**: 2777–2784.

32 Vite, CH, McGowan, JC, Niogi, SN, Passini, MA, Drobatz, KJ, Haskins, ME *et al.* (2005). Effective gene therapy for an inherited CNS disease in a large animal model. *Ann Neurol* **57**: 355–364.

33 Passini, MA, Watson, DJ, Vite, CH, Landsburg, DJ, Feigenbaum, AL and Wolfe, JH (2003). Intraventricular brain injection of adeno-associated virus type 1 (AAV1) in neonatal mice results in complementary patterns of neuronal transduction to AAV2 and total long-term correction of storage lesions in the brains of beta-glucuronidase-deficient mice. *J Virol* **77**: 7034–7040.

34 Hadaczek, P, Eberling, JL, Pivirotto, P, Bringas, J, Forsayeth, J and Bankiewicz, KS (2010). Eight years of clinical improvement in MPTP-lesioned primates after gene therapy with AAV2-hAADC. *Mol Ther* **18**: 1458–1461.

35 Fukuyama, H, Hayashi, T, Katsumi, Y, Tsukada, H and Shibasaki, H (1998). Issues in measuring glucose metabolism of rat brain using PET: the effect of harderian glands on the frontal lobe. *Neurosci Lett* **255**: 99–102.

36 Hume, SP, Lammertsma, AA, Myers, R, Rajeswaran, S, Bloomfield, PM, Ashworth, S *et al.* (1996). The potential of high-resolution positron emission tomography to monitor striatal dopaminergic function in rat models of disease. *J Neurosci Methods* **67**: 103–112.

37 Kuge, Y, Minematsu, K, Hasegawa, Y, Yamaguchi, T, Mori, H, Matsuura, H *et al.* (1997). Positron emission tomography for quantitative determination of glucose metabolism in normal and ischemic brains in rats: an insoluble problem by the Harderian glands. *J Cereb Blood Flow Metab* **17**: 116–120.

38 Husain, T, Passini, MA, Parente, MK, Fraser, NW and Wolfe, JH (2009). Long-term AAV vector gene and protein expression in mouse brain from a small pan-cellular promoter is similar to neural cell promoters. *Gene Ther* **16**: 927–932.

39 Yu, Y, Annala, AJ, Barrio, JR, Toyokuni, T, Satyamurthy, N, Namavari, M *et al.* (2000). Quantification of target gene expression by imaging reporter gene expression in living animals. *Nat Med* **6**: 933–937.

40 Slifstein, M, Kegeles, LS, Xu, X, Thompson, JL, Urban, N, Castrillon, J *et al.* (2010). Striatal and extrastriatal dopamine release measured with PET and [(18)F] fallypride. *Synapse* **64**: 350–362.

41 Mukherjee, J, Yang, ZY, Lew, R, Brown, T, Kronmal, S, Cooper, MD *et al.* (1997). Evaluation of d-amphetamine effects on the binding of dopamine D-2 receptor radioligand, ^{18}F-fallypride in nonhuman primates using positron emission tomography. *Synapse* **27**: 1–13.

42 Leung, K (2005). 3-N-(2-[^{18}F]fluoroethyl)spiperone. *Molecular Imaging and Contrast Agent Database (MICAD) [internet]: 2004–2013*. National Center for Biotechnology Information: Bethesda, MD.

43 Mukherjee, J, Christian, BT, Dunigan, KA, Shi, B, Narayanan, TK, Satter, M *et al.* (2002). Brain imaging of ^{18}F-fallypride in normal volunteers: blood analysis, distribution, test-retest studies, and preliminary assessment of sensitivity to aging effects on dopamine D-2/D-3 receptors. *Synapse* **46**: 170–188.

44 Mukherjee, J, Yang, ZY, Brown, T, Lew, R, Wernick, M, Ouyang, X *et al.* (1999). Preliminary assessment of extrastriatal dopamine D-2 receptor binding in the rodent and nonhuman primate brains using the high affinity radioligand, ^{18}F-fallypride. *Nucl Med Biol* **26**: 519–527.

45 Nagano-Saito, A, Dagher, A, Booij, L, Gravel, P, Welfeld, K, Casey, KF *et al.* (2013). Stress-induced dopamine release in human medial prefrontal cortex–^{18}F-fallypride/PET study in healthy volunteers. *Synapse* **67**: 821–830.

46 Yaghoubi, SS, Jensen, MC, Satyamurthy, N, Budhiraja, S, Paik, D, Czernin, J *et al.* (2009). Noninvasive detection of therapeutic cytolytic T cells with ^{18}F-FHBG PET in a patient with glioma. *Nat Clin Pract Oncol* **6**: 53–58.

47 Maresz, K, Carrier, EJ, Ponomarev, ED, Hillard, CJ and Dittel, BN (2005). Modulation of the cannabinoid CB2 receptor in microglial cells in response to inflammatory stimuli. *J Neurochem* **95**: 437–445.

48 Yaghoubi, S, Barrio, JR, Dahlbom, M, Iyer, M, Namavari, M, Satyamurthy, N *et al.* (2001). Human pharmacokinetic and dosimetry studies of [(18)F]FHBG: a reporter probe for imaging herpes simplex virus type-1 thymidine kinase reporter gene expression. *J Nucl Med* **42**: 1225–1234.

49 Ogawa, O, Umegaki, H, Ishiwata, K, Asai, Y, Ikari, H, Oda, K *et al.* (2000). *In vivo* imaging of adenovirus-mediated over-expression of dopamine D2 receptors in rat striatum by positron emission tomography. *Neuroreport* **11**: 743–748.

50 Lock, M, Alvira, M, Vandenberghe, LH, Samanta, A, Toelen, J, Debyser, Z *et al.* (2010). Rapid, simple, and versatile manufacturing of recombinant adeno-associated viral vectors at scale. *Hum Gene Ther* **21**: 1259–1271.

51 Passini, MA and Wolfe, JH (2001). Widespread gene delivery and structure-specific patterns of expression in the brain after intraventricular injections of neonatal mice with an adeno-associated virus vector. *J Virol* **75**: 12382–12392.

52 Cearley, CN, Vandenberghe, LH, Parente, MK, Carnish, ER, Wilson, JM and Wolfe, JH (2008). Expanded repertoire of AAV vector serotypes mediate unique patterns of transduction in mouse brain. *Mol Ther* **16**: 1710–1718.

53 Cearley, CN and Wolfe, JH (2007). A single injection of an adeno-associated virus vector into nuclei with divergent connections results in widespread vector distribution in the brain and global correction of a neurogenetic disease. *J Neurosci* **27**: 9928–9940.